JACS
JOURNAL OF THE AMERICAN CHEMICAL SOCIETY
Article
pubs.acs.org/JACS

Supramolecular Assembly of Multicomponent Photoactive Systems via Cooperatively Coupled Equilibria

Miguel García-Iglesias,[†,∥] Katrin Peuntinger,[‡] Axel Kahnt,[‡] Jan Krausmann,[‡] Purificación Vázquez,[†] David González-Rodríguez,*[,†] Dirk M. Guldi,*[,‡] and Tomás Torres*[,†,§]

[†]Departamento de Química Orgánica, Facultad de Ciencias, Universidad Autónoma de Madrid, 28049 Madrid, Spain
[‡]Department of Chemistry and Pharmacy and Interdisciplinary Center for Molecular Materials (ICMM), Friedrich-Alexander-Universität Erlangen-Nürnberg, Egerlandstrasse 3, 91058 Erlangen, Germany
[§]IMDEA Nanociencia, Universidad Autónoma de Madrid, c/Faraday 9, Campus de Cantoblanco, 28049 Madrid, Spain

Supporting Information

ABSTRACT: Here, we show that the synergistic interplay between two binding equilibria, acting at different sites of a (Zn)phthalocyanine-amidine molecule (**Pc1**), enables the dissociation of the photoinactive phthalocyanine dimer $(\mathbf{Pc1})_2$ into a three-component system, in which a sequence of light harvesting, charge separation, and charge shift is successfully proven. The aforementioned dimer is assembled by dual amidine-Zn(II) coordination between neighboring **Pc1** molecules and gives rise to high association constants ($K_D \approx 10^{11}$ M^{-1}). Such extraordinary stability hampers the individual binding of either carboxylic acid ligands through the amidine group or pyridine-type ligands through the Zn(II) metal atom to $(\mathbf{Pc1})_2$. However, the combined addition of both ligands, which cooperatively bind to different sites of **Pc1** through distinct noncovalent interactions, efficiently shifts the overall equilibrium toward a photoactive tricomponent species. In particular, when a fullerene-carboxylic acid ($\mathbf{C_{60}A}$) and either a dimethylamino-pyridine (**DMAP**) or a phenothiazine-pyridine ligand (**PTZP**) are simultaneously present, the photoactivity is turned on and evidence is given for an electron transfer from photoexcited **Pc1** to the electron-accepting $\mathbf{C_{60}A}$ that affords the **DMAP-Pc1**$^{\bullet+}$-$\mathbf{C_{60}A}^{\bullet-}$ or **PTZP-Pc1**$^{\bullet+}$-$\mathbf{C_{60}A}^{\bullet-}$ radical ion pair states. Only in the latter case does a cascade of photoinduced electron transfer processes afford the **PTZP**$^{\bullet+}$-**Pc1**-$\mathbf{C_{60}A}^{\bullet-}$ radical ion pair state. The latter is formed via a thermodynamically driven charge shift evolving from **PTZP-Pc1**$^{\bullet+}$-$\mathbf{C_{60}A}^{\bullet-}$ and exhibits lifetimes that are notably longer than those of **DMAP-Pc1**$^{\bullet+}$-$\mathbf{C_{60}A}^{\bullet-}$.

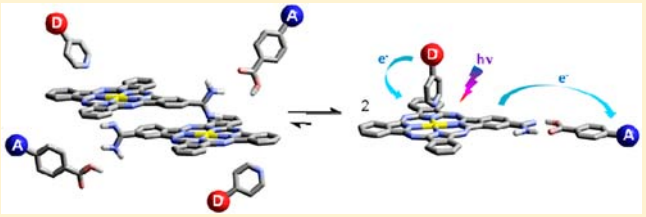

1. INTRODUCTION

Cooperative interactions constitute a fundamental mechanism to modulate the behavior of complex molecular systems.[1] Allosteric cooperativity between a host and an effector molecule, in particular, plays a ubiquitous role in nature to regulate substrate binding[2] or protein polymerization[3] by means of changes in the host protein conformation and/or oligomeric state.[4] The effector can either enhance (*positive* allosterism) or diminish (*negative* allosterism) the subsequent binding of the same (*homotropic* allosterism) or a different chemical species (*heterotropic* allosterism) to the host.

The ultimate consequence arising from the interplay between several chemical species binding at different host sites is that the system activity, as a whole, is turned either *on* or *off*. Such activity can be very diverse. Chemists in particular have developed numerous artificial supramolecular systems that model the complex cooperative behavior of biological systems, focusing mainly on catalytic or sensing activity.[5]

Here, we describe a system where cooperatively coupled equilibria between a host phthalocyanine (Pc)[6] dimer and two different ligands leads to well-defined tricomponent supramolecular assemblies displaying light harvesting, charge separation, and charge shift activity. The *off* state is a monoamidine-Pc cofacial dimer ($(\mathbf{Pc1})_2$) stabilized by dual coordination of the amidine group of one Pc molecule to the Zn(II) central atom of the adjacent Pc molecule, as shown in Scheme 1. The aforementioned dimer exhibits extraordinary stability in solution and does not dissociate in the presence of equivalent amounts of either carboxylic acids (A, binding to the amidine group) or pyridine ligands (P, binding to the Zn(II) centers). However, the combined action of both ligands leads to the *on* state in an "all or nothing" process, where full dissociation of $(\mathbf{Pc1})_2$ yields a P-**Pc1**-A tricomponent species. In the latter, after **Pc1** photoexcitation a cascade of short-range electron transfer processes creates a long-lived radical ion pair state (Scheme 1).[7] As such, the resulting three-component system mimics all of the individual steps seen in the photosynthetic reaction center. In particular, a broad absorption cross section in the range of maximum solar flux enables efficient light harvesting, fast charge separation to yield

Received: October 2, 2013
Published: December 16, 2013

dx.doi.org/10.1021/ja410114d | J. Am. Chem. Soc. 2013, 135, 19311−19318

Scheme 1. Chemical Structures and Equilibria Involved in This Work

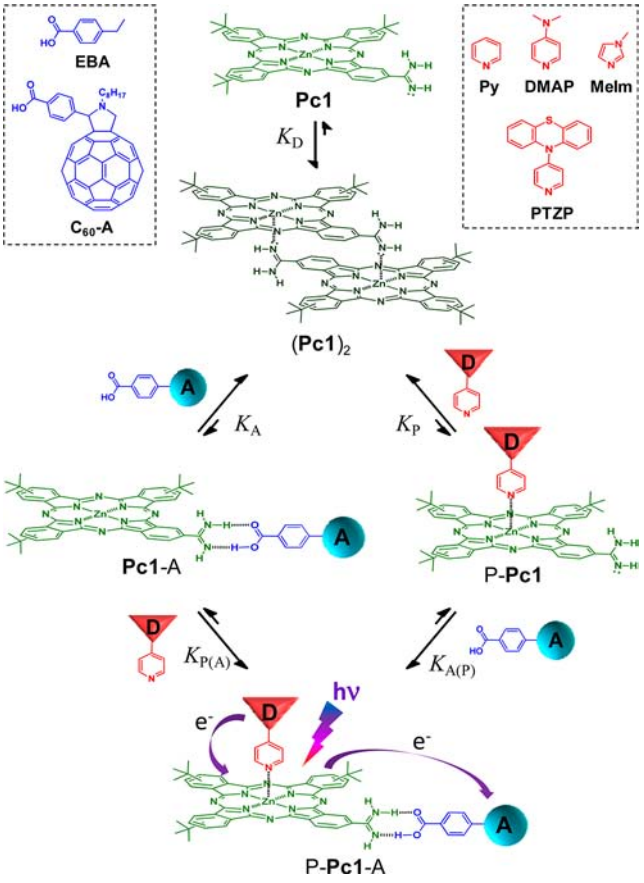

an adjacent radical ion pair state, and charge shift to transform the latter into a distant radical ion pair state.[8]

2. RESULTS AND DISCUSSION

2.1. Study of the Supramolecular Equilibria. The synthetic route toward **Pc1**,[9] **C_{60}A**,[10] and **PTZP**[11] is described in the Supporting Information (Schemes S1−S3).

The self-association behavior of **Pc1** was first examined by absorption, fluorescence, and ESI MS measurements. These experiments revealed the formation of a J-type cofacial dimer ($(\mathbf{Pc1})_2$) in apolar solvents by double amidine-Zn coordination. For instance, the first feature to be noticed in the absorption spectra in noncoordinating solvents ($CHCl_3$, toluene) relative to typical Zn-coordinating solvents (pyridine, THF), is the presence of split Q-bands at 671 and 700 nm (Figure 1). These features resemble those of related Pc-imidazole cofacial dimers described by Kobuke et al.,[12,13] in which Q-band splitting was attributed to exciton interactions that evoke red-shifted Q_x and blue-shifted Q_y-bands. The self-association of **Pc1** was confirmed by ESI Q-TOF MS experiments, where the most prominent peak at m/z 1577.6 is assigned to the $[(\mathbf{Pc1})_2]^+$ ion (Figure S1, Supporting Information). ^{1}H NMR titration experiments were also performed to gain further insight into the different supramolecular equilibria. Although the trends observed support our hypotheses, the NMR signals are too broad to enable reliable conclusions.

$(\mathbf{Pc1})_2$ exhibits an extraordinary stability to concentration or temperature changes. For example, diluting toluene solutions of $(\mathbf{Pc1})_2$ from 10^{-4} to 10^{-8} M or heating them to 90 °C did not

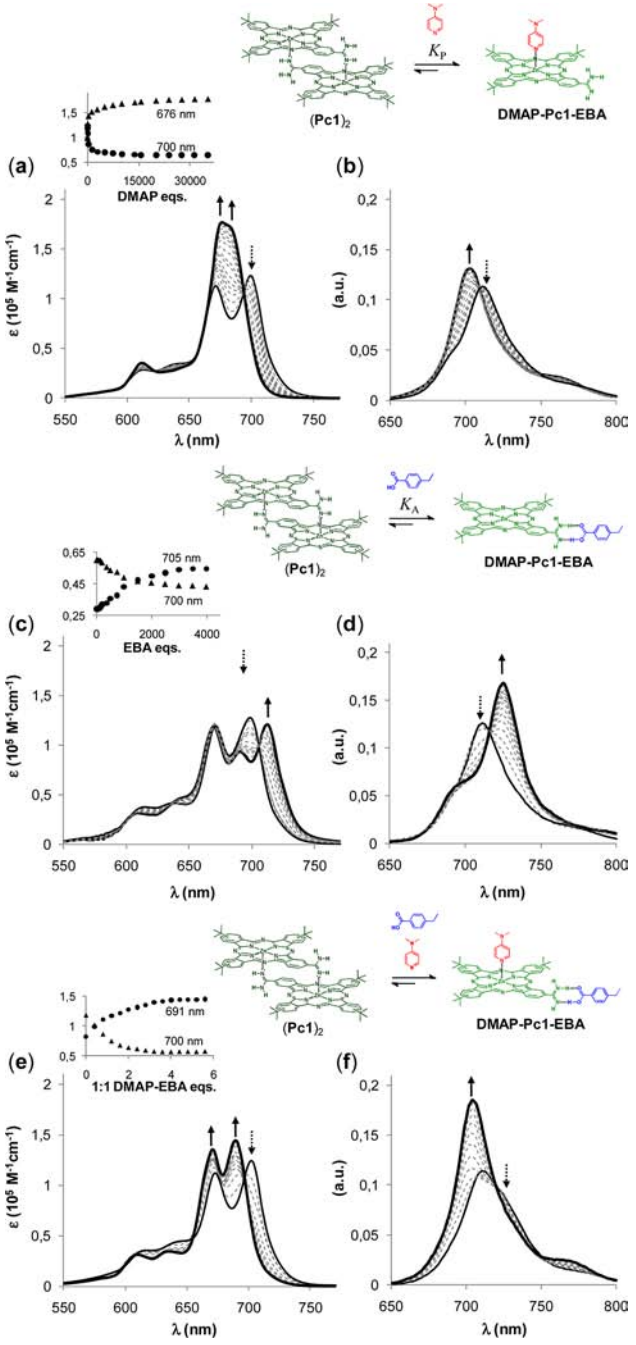

Figure 1. **Pc1** ($[\mathbf{Pc1}] = 8 \times 10^{-6}$ M in toluene) Q-band absorption (a, c, e) and emission (b, d, f) changes observed upon addition of **DMAP** (up to 3.5×10^5 equiv; a, b), **EBA** (up to 4×10^4 equiv; c, d), and a 1:1 mixture of **DMAP** and **EBA** (up to 6 equiv; e, f). In the emission spectra (b, d, f), samples were excited at isosbestic points 599, 599, and 597 nm, respectively. Insets in a, c, e: absorption changes at a given wavelength as a function of ligand equivalents.

lead to any appreciable spectral changes (Figure S2, Supporting Information). From these spectroscopic assays we also discard further aggregation of $(\mathbf{Pc1})_2$ by coordination or $\pi-\pi$ interactions within these concentration and temperature ranges.[14]

$(\mathbf{Pc1})_2$ was first subjected to competition experiments with Zn-binding ligands. Titration of $(\mathbf{Pc1})_2$ toluene solutions with pyridine (**Py**), dimethylamino-pyridine (**DMAP**) (see Figure 1), or methylimidazole (**MeIm**) (see Figure S3, Supporting

dx.doi.org/10.1021/ja410114d | J. Am. Chem. Soc. 2013, 135, 19311−19318

Information) revealed that adding small amounts of these ligands (up to ca. 100 equiv) resulted in no significant spectral changes. However, upon adding a larger amount of the ligand the characteristic $(\mathbf{Pc1})_2$ split Q-bands gradually converge to a species that features two close maxima at 676 and 684 nm (Figure 1a) and that matches the spectrum of **Pc1** in pyridine or THF. The final stationary state, reached through isosbestic points at 599, 623, 658, and 694 nm, could only be observed after the addition of ca. 10^4-10^5 equiv of **Py**, **DMAP**, or **MeIm**. As a matter of fact, these spectral changes are attributed to the dissociation of $(\mathbf{Pc1})_2$ by means of a competition with Zn-coordinating ligands (P) to yield P-**Pc1** (K_P; Scheme 1). In steady-state fluorescence measurements, a similar trend was noticed (Figure 1b). Mirror-imaged to the long wavelength absorption maximum, $(\mathbf{Pc1})_2$ reveals a fluorescence maximum at 710 nm and a fluorescence quantum yield of 0.12.[15] Again, this fluorescence band is insensitive to the presence of a few equivalents of Zn-coordinating ligands and to temperature. Only in the presence of larger amounts, and again up to 10^4-10^5 ligand equiv, do the fluorescence features gradually shift to 701 nm, while their intensity is slightly increased by a factor of 1.16.

From the aforementioned titration experiments we derived dimerization constants (K_D) for **Pc1** to transform into $(\mathbf{Pc1})_2$ in toluene of 3.4×10^{11} M^{-1} in terms of absorption and 1.6×10^{11} M^{-1} in terms of fluorescence (see Figure S6, Supporting Information). Such extraordinary stability is comparable to that obtained for related Pc-imidazole derviatives.[13] They reflect the remarkable strength of these J-type dimers with double complementary coordination, especially in comparison to the association constants of related ZnPc species with pyridine or imidazole ligands, which are in the range of 10^3-10^5 in apolar solvents.[16]

Next, we turned our attention to the effect of adding carboxylic acids (A) to $(\mathbf{Pc1})_2$ solutions (K_A; Scheme 1). Amidines are known to strongly bind to carboxylic acids through hydrogen-bonding and electrostatic interactions with association constants on the order of 10^5-10^7 M.[17,18] It is notable that such a binding motif has been employed to control through-bond-mediated electron transfer processes between electron donors and electron acceptors.[18] Despite the strong association, the addition of a small excess (i.e., <50 equiv) of 4-ethylbenzoic acid (**EBA**) to toluene solutions of $(\mathbf{Pc1})_2$ failed again to evoke any significant dimer dissociation. In line with the titration measurements with Zn-coordinating ligands (vide supra) clear absorption and fluorescence changes were only observed after the addition of 100 **EBA** equiv. Further **EBA** addition, that is, up to 3×10^3 equiv, led to a stationary state, whose spectral features are quite different from those described above, since the supposed ZnPc final species is also different (P-**Pc1** vs **Pc1**-A; see Scheme 1). In particular, the red-shifted dimer Q-band at 700 nm splits into two new maxima at 689 and 711 nm, while the dimer Q-band at 671 nm blue-shifts only slightly to 667 nm (see Figure 1c). Throughout the titration with **EBA**, isosbestic points were found at 599, 636, 669, and 705 nm, sustaining the assumption of an equilibrium between $(\mathbf{Pc1})_2$ and **Pc1**-**EBA**.

In similar titrations with $(\mathbf{Pc1})_2$, but monitored through means of fluorescence (Figure 1d), the maximum red-shifts to 724 nm and the fluorescence intensity increases by a factor of 1.35 upon formation of **Pc1**-**EBA**. These red-shifted absorption and fluorescence bands are in fact characteristic of amidine complexations with acids. They were attributed by Nocera et al. to electronic effects arising upon protonation/acid coordination when the amidine group is conjugated with the macrocycle.[18a]

In short, taking the magnitude of the dimerization constant of **Pc1** ($K_D \approx 10^{11}$ M^{-1}) into account, it is reasonable to assume that $(\mathbf{Pc1})_2$ lacks meaningful affinities toward binding carboxylic acids (through the amidine group; $K_A < 1$) or pyridines (through the Zn metal atom; $K_P < 1$). However, the combined addition of both ligands, binding to different sites of **Pc1**, seems to efficiently shift the overall equilibrium toward the formation of a P-**Pc1**-A three-component species (see Scheme 1).[19] Figure 1e, f documents absorption and emission titration experiments regarding $(\mathbf{Pc1})_2$ in the presence of up to 6 equiv of both **DMAP** and **EBA**. The overall trend and the final spectra do not resemble those seen in the titrations with either an excess of **DMAP** or **EBA**. Now, the dimer Q-band absorption at 671 nm red-shifts only slightly to 672 nm, whereas the band at 700 nm shifts to 691 nm. Isosbestic points were found at 597, 609, 655, and 696 nm, strongly supporting an equilibrium between two Pc-containing species: that is, $(\mathbf{Pc1})_2$ and the three-component system **DMAP**-**Pc1**-**EBA**. On the other hand, during these titrations the fluorescence maximum blue-shifts to 704 nm and its intensity is enhanced by a factor of 1.60 with respect to $(\mathbf{Pc1})_2$. In complementary ESI Q-TOF experiments in the presence of a small excess of both **DMAP** and **EBA**, we could not detect the peak corresponding to **DMAP**-**Pc1**-**EBA**. Instead, the [**DMAP**-**Pc1**+H]$^+$ charged species was detected at m/z 909.4 in the positive ion mode (see Figure S1, Supporting Information).

It is interesting to note that the same stationary states in terms of absorption and/or fluorescence were realized by going through clear isosbestic points when choosing any other **DMAP**/**EBA** addition order (see Figure S8, Supporting Information). For instance, adding only a small excess (10 equiv) of one of the ligands (**DMAP** or **EBA**), which evokes no discernible spectral changes, and then exceeding just 1 equiv of the other ligand (**EBA** or **DMAP**, respectively) result in the same final **DMAP**-**Pc1**-**EBA** spectra (see Figure S8, Supporting Information). The latter observations underline the cooperative nature of these equilibria. From these titration experiments we derived the apparent binding constants between **DMAP** ($K_{P(A)}$) or **EBA** ($K_{A(P)}$) and **Pc1** in solutions containing a 10-fold excess of the complementary ligands; namely **EBA** and **DMAP**. The values derived are $K_{P(A)} = 6.4 \times 10^4$ M^{-1} and $K_{A(P)} = 2.8 \times 10^5$ M^{-1} when analyzing the absorption changes, as well as $K_{P(A)} = 6.0 \times 10^4$ M^{-1} and $K_{A(P)} = 1.2 \times 10^5$ M^{-1} when considering the fluorescence measurements.[20]

The unique behavior of $(\mathbf{Pc1})_2$, that is, being nonresponsive to either carboxylic acids or pyridines but being responsive to their combined addition, prompted us to probe an electron-donating phenothiazine in the pyridine ligand (**PTZP**) and an electron-accepting C_{60} in the carboxylic acid ligand ($\mathbf{C_{60}A}$). Titration experiments similar to those shown in Figure 1 were carried out with **PTZP** and $\mathbf{C_{60}A}$ (Figure 2). Notably, the results are virtually identical with those obtained with **DMAP** and **EBA** in terms of absorption changes and ligand concentrations required to reach the stationary states. Changes in the fluorescence were, however, very different. In all of the cases the **Pc1** fluorescence is significantly quenched relative to $(\mathbf{Pc1})_2$—a trend that is likely due to electron transfer within the complexes (vide infra).

To rationalize the photophysics of **PTZP**-**Pc1**-$\mathbf{C_{60}A}$, including electron transfer processes, we initially focused on a reference system containing only two electron transfer active

dx.doi.org/10.1021/ja410114d | J. Am. Chem. Soc. 2013, 135, 19311−19318

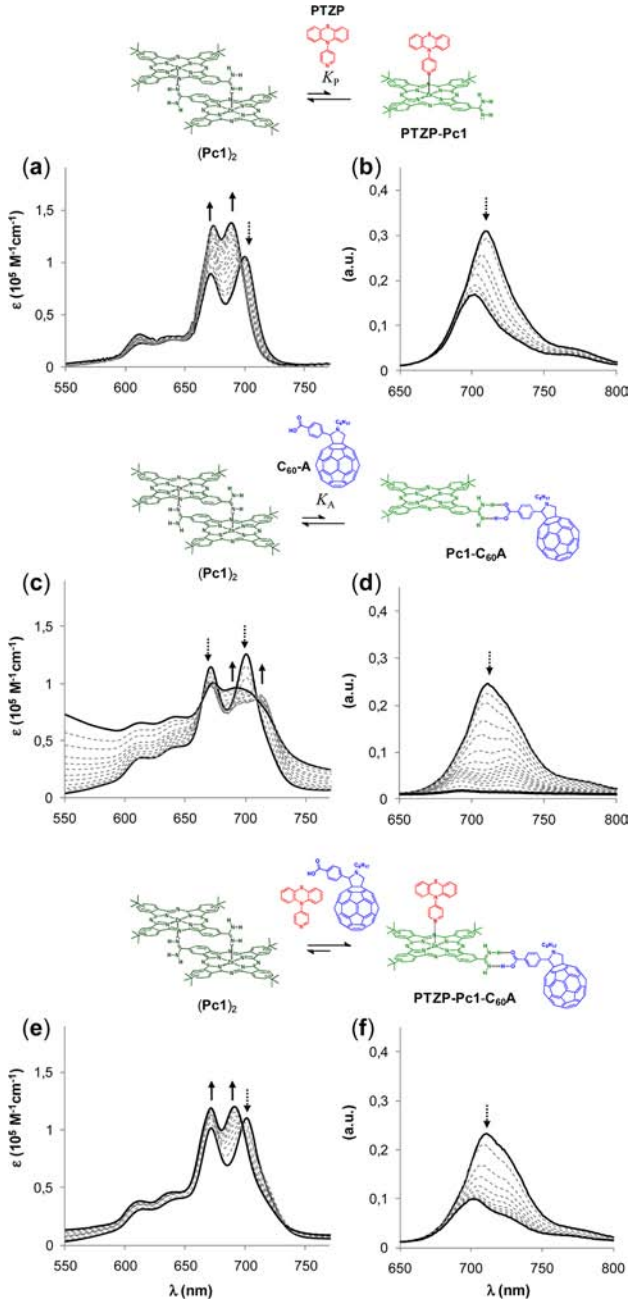

Figure 2. Pc1 ([**Pc1**] = 8×10^{-6} M) Q-band absorption (a, c, e) and emission (b, d, f) changes that occur upon addition of **PTZP** (up to 3×10^5 equiv; a, b), C_{60}-A (up to 5×10^4 equiv; c, d), and a 1:1 mixture of **PTZP** and $\mathbf{C_{60}A}$ (up to 6 equiv; e, f) in toluene. In the emission spectra (b, d, f) samples were excited at 599, 599, and 597 nm, respectively.

units, namely **Pc1** and $\mathbf{C_{60}A}$. This was performed by titrating $(\mathbf{Pc1})_2$ toluene solutions containing a small excess (4 equiv) of **DMAP** with $\mathbf{C_{60}A}$ (from 0 up to 9 equiv). In the stationary state, which was realized upon adding ca. 4 $\mathbf{C_{60}A}$ equiv, the **DMAP-Pc1-**$\mathbf{C_{60}A}$ complex ($K_{A(P)}$; Scheme 1) is present as the main **Pc1** species in solution. Hence, a 4:1:4 **DMAP:Pc1:**$\mathbf{C_{60}A}$ ratio was considered optimal to reach close to quantitative formation of the three-component system. It is interesting that the Q-band absorptions (Figure S9, Supporting Information) experienced the same isosbestic points and blue shifts as in the titration with **DMAP** and **EBA** (please compare, Figure 1e and Figure S8, Supporting Information), namely from 614 to 611 nm, from 640 to 635 nm, and from 700 to 693 nm, which supports the equilibrium between $(\mathbf{Pc1})_2$ and **DMAP-Pc1-**$\mathbf{C_{60}A}$. First insights into excited state interactions between **Pc1** and $\mathbf{C_{60}A}$ in **DMAP-Pc1-**$\mathbf{C_{60}A}$ came from steady-state fluorescence measurements. The **Pc1** fluorescence reveals a blue shift to 701 nm and an exponential quenching with increasing $\mathbf{C_{60}A}$ concentration up to 70% in the stationary state. These titrations in the presence of **DMAP** were used to evaluate the **Pc1:**$\mathbf{C_{60}A}$ apparent binding constant $K_{A(P)}$ (Figure S10, Supporting Information), which amounts to 4.0×10^4 M^{-1} and compares reasonably well with the $K_{A(P)}$ value obtained with **Pc1** and **EBA** (Figure S8, Supporting Information). From these fluorescence experiments we also constructed a Job plot (Figure S11, Supporting Information), which affords a slope change at a molar fraction of 0.5 and, in turn, confirms the 1:1 **Pc1:**$\mathbf{C_{60}A}$ complex stoichiometry in **DMAP-Pc1-**$\mathbf{C_{60}A}$.

As a complement to the aforementioned studies, time-resolved fluorescence measurements were carried out. In particular, 647 nm was chosen as an excitation wavelength to ensure the selective excitation of **Pc1** in **DMAP-Pc1-**$\mathbf{C_{60}A}$, in combination with a detection wavelength of 700 nm. In the absence of **DMAP** or $\mathbf{C_{60}A}$, $(\mathbf{Pc1})_2$ had a fluorescence lifetime of 2.71 ns. No appreciable lifetime changes were seen upon adding a small excess of **DMAP**. Difference emerged again, however, when **DMAP** and $\mathbf{C_{60}A}$ were both present (Figure S12, Supporting Information). In general, the fluorescence decays were best fit by a two-exponential fitting function. The longer lifetime, that is 2.3 ± 0.2 ns, correlates to free $(\mathbf{Pc1})_2$, while the shorter lifetime of 0.34 ± 0.02 ns is due to the fluorescence deactivation in **DMAP-Pc1-**$\mathbf{C_{60}A}$. The latter is in perfect agreement with the fluorescence quenching when quantitative complexation is realized (vide supra). The equilibrium between $(\mathbf{Pc1})_2$ and **DMAP-Pc1-**$\mathbf{C_{60}A}$ is reassured by the fact that the relative amplitude of the longer-lived component (2.3 ns) decreased as the $\mathbf{C_{60}A}$ concentration increased, while that of the shorter-lived component (0.34 ns) increased simultaneously until reaching again a 4:1:4 **DMAP:Pc1:**$\mathbf{C_{60}A}$ ratio.

Next, we turned to transient absorption measurements. First, the references, that is $(\mathbf{Pc1})_2$—with and without **DMAP**—and $\mathbf{C_{60}A}$ were probed. Upon 660 nm excitation of $(\mathbf{Pc1})_2$, we noticed that within less than 2.0 ps the lowest singlet excited state is formed via rapid deactivation of higher lying excited states (Figure S13, Supporting Information). In particular, characteristic maxima at 500, 595, 625, 760, and 830 nm, as well as minima at 610, 640, 670, and 700 nm, relate to $(\mathbf{Pc1})_2$ singlet−singlet absorptions. On a time scale of up to 3000 ps the fate of the $(\mathbf{Pc1})_2$ singlet excited state is intersystem crossing (3.0 ns / 3.3×10^8 s^{-1}) to transform the singlet into the corresponding triplet excited state. The latter was characterized by a long-lived (76 μs / 1.3×10^4 s^{-1}) and strongly absorbing triplet−triplet transition at 500 nm. Addition of **DMAP** led again to no appreciable changes—either in terms of spectroscopic features or in terms of kinetic features. On the other hand, 387 nm excitation of $\mathbf{C_{60}A}$ (not shown) populates the corresponding singlet excited state, with its characteristic absorption maximum at 895 nm. The $\mathbf{C_{60}A}$ singlet excited state is short-lived (1.2 ns / 8.3×10^8 s^{-1}) as it undergoes intersystem crossing to the triplet manifold with a characteristic maximum at 700 nm.[21]

Then, the transient absorption changes of **DMAP-Pc1-**$\mathbf{C_{60}A}$, obtained at the optimal 4:1:4 **DMAP:Pc1:**$\mathbf{C_{60}A}$ relative ratio

dx.doi.org/10.1021/ja410114d | J. Am. Chem. Soc. 2013, 135, 19311−19318

(vide supra), were recorded with several time delays after 660 nm laser excitation (Figure 3) and compared with those seen for $(\mathbf{Pc1})_2$. This is meant to address exclusively **DMAP-Pc1-C_{60}A** rather than any other species in solution.

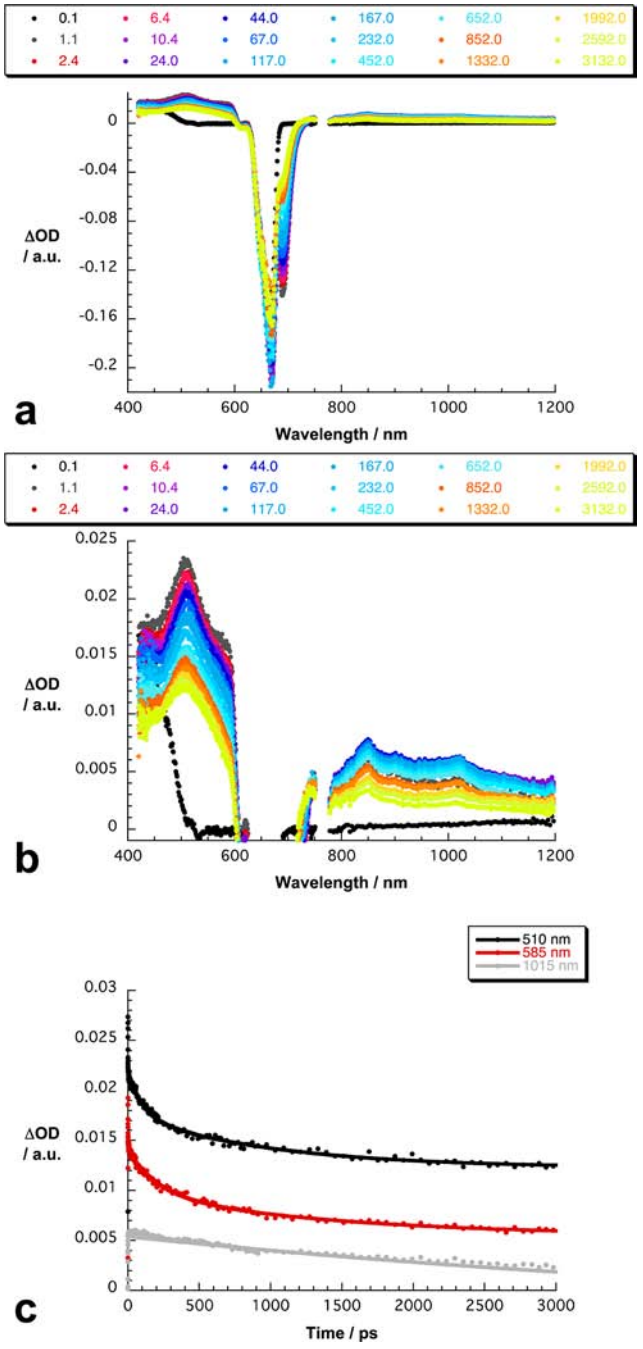

Figure 3. (a) Differential absorption spectra (visible and near-IR) obtained upon femtosecond flash photolysis (660 nm) of **DMAP-Pc1-C_{60}A** (4:1:4) in toluene with several time delays between 0.1 (black spectrum) and 3032.0 ps (yellow spectrum) at room temperature. (b) Zoom in into differential absorption spectra (visible and near-IR) obtained upon femtosecond flash photolysis (660 nm) of **DMAP-Pc1-C_{60}A** (4:1:4) in toluene with several time delays between 0.1 (black spectrum) and 3032.0 ps (yellow spectrum) at room temperature. (c) Time absorption profiles of the spectra shown above at 510/585 nm (**Pc1** radical cation) and 1015 nm (C_{60}A radical anion) monitoring the charge separation and the charge recombination.

At early times, that is, up to 50 ps, the transient features include strong maxima at 505, 590, 625, and 840 nm, as well as minima at 610, 640, 670, and 690 nm, which are practically identical with those seen for $(\mathbf{Pc1})_2$. The only appreciable differences are the blue-shifted minima—due to Q-band bleaching—that are found in **DMAP-Pc1-C_{60}A** at 690 nm. In contrast to the case for $(\mathbf{Pc1})_2$, all of the singlet excited state characteristics are subject to a fast decay. From multiwavelength analyses the singlet excited state lifetime was determined to be 0.35 ± 0.07 ns. Simultaneously, a new transient evolves in the visible region, that is, a maximum at 510 nm and minima at 670 and 690 nm, and in the near-infrared, with maxima at 755, 845, and 1015 nm. A spectral comparison with pulse radiolytic and electrochemical data suggests that the maxima at 510, 755, and 845 nm relate to the **Pc1** π-radical cation ($\mathbf{Pc1}^{\bullet+}$) fingerprint, while the maximum at 1015 nm corresponds to the C_{60}**A** π-radical anion ($C_{60}\mathbf{A}^{\bullet-}$) signature.[22]

In conclusion, our results attest to the successful charge separation in the complex as it evolves from the **Pc1** singlet excited state to the electron-accepting C_{60}**A** to yield the **DMAP-Pc1**$^{\bullet+}$**-C_{60}A**$^{\bullet-}$ radical ion pair state.[23] The **DMAP-Pc1**$^{\bullet+}$**-C_{60}A**$^{\bullet-}$ absorption is stable on the femto- and picosecond time scale but decays on the nanosecond regime. From complementary nanosecond experiments we have derived a **DMAP-Pc1**$^{\bullet+}$**-C_{60}A**$^{\bullet-}$ radical ion pair state lifetime of 10 ns (Figure S14, Supporting Information). It is interesting to note that charge recombination populates the **Pc1** triplet excited state (Figure S15, Supporting Information), which features lifetimes of 70 μs and 60 ns in the absence and in the presence of molecular oxygen, respectively. To determine the **Pc1** triplet quantum yield, singlet oxygen fluorescence, which is formed in the latter reaction, is measured. The fact that photoexcitation of **Pc1** and **DMAP**, in the presence of variable concentrations of C_{60}**A**, resulted in singlet oxygen formation higher than that in the absence of any C_{60}**A** suggests that charge recombination leads to the quantitative formation of the **Pc1** triplet excited state (Figure S16, Supporting Information).

Finally, we probed **PTZP-Pc1-C_{60}A**, now containing three electroactive species, under the same conditions. Parts e and f of Figure 2 show respectively the **Pc1** Q-band absorption and fluorescence changes that occur upon titrating $(\mathbf{Pc1})_2$ with a 1:1 mixture of **PTZP** and C_{60}**A** in toluene. Again, total complexation was observed after a **PTZP:Pc1:C_{60}A** 4:1:4 ratio was reached. Please note the similarity in *Q*-band absorption changes shown in Figures 1e and 2e and Figure S9 (Supporting Information), which suggests that **Pc1** is involved with **PTZP** and C_{60}**A** in similar equilibria as with **DMAP** and **EBA** or with **DMAP** and C_{60}**A**. The fluorescence is, however, significantly quenched at the end of the titrations that were performed with **PTZP** and C_{60}**A**—compare Figures 1f and 2f. As a matter of fact, fluorescence changes with respect to blue shifts and quenching similar to those seen for **DMAP-Pc1-C_{60}A** (Figure S10, Supporting Information) were obtained in the titrations leading toward **PTZP-Pc1-C_{60}A** (Figure 2f). This suggests that upon photoexcitation **Pc1** and C_{60}**A** are subject to the same charge transfer process as discussed above.

In terms of transient absorption changes, **PTZP-Pc1-C_{60}A** and **DMAP-Pc1-C_{60}A** revealed identical charge separation reactivity and kinetics (Figure 4), which is in good agreement with our results in the fluorescence measurements. However, on the nanosecond time scale (Figure 5) the initially formed **PTZP-Pc1**$^{\bullet+}$**-C_{60}A**$^{\bullet-}$ deactivates via a charge shift to **PTZP** rather than triplet excited state formation, due to the lower

dx.doi.org/10.1021/ja410114d | J. Am. Chem. Soc. 2013, 135, 19311−19318

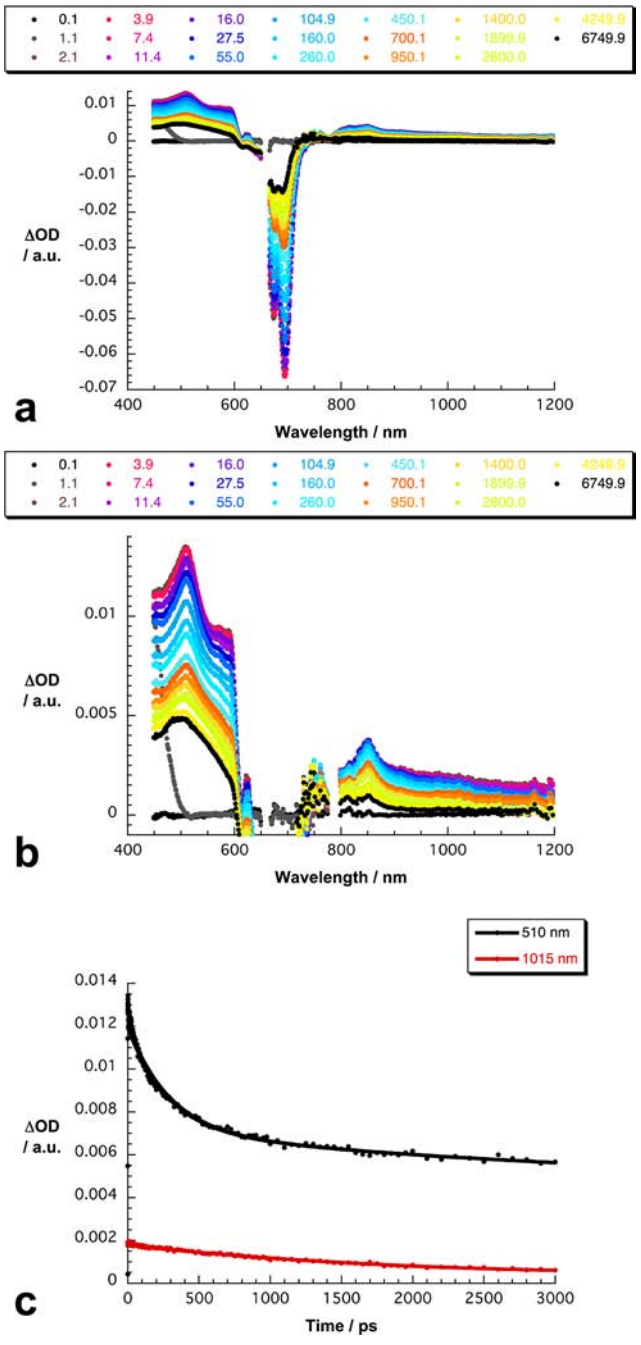

Figure 4. (a) Differential absorption spectra (visible and near-IR) obtained upon femtosecond flash photolysis (660 nm) of **PTZP-Pc1-C_{60}A** (4:1:4) in toluene with several time delays between 0.1 and 6749.9 ps at room temperature. (b) Zoom into differential absorption spectra (visible and near-IR) obtained upon femtosecond flash photolysis (660 nm) of **PTZP-Pc1-C_{60}A** (4:1:4) in toluene with several time delays between 0.1 and 6749.9 ps at room temperature. (c) Time absorption profiles of the spectra shown above at 510 nm (**Pc1** radical cation) and 1015 nm (C_{60}**A** radical anion) monitoring the charge separation and the charge shift.

oxidation potential of phenothiazine relative to Pc.[24] In the correspondingly formed **PTZP**$^{\bullet+}$**-Pc1-C_{60}A**$^{\bullet-}$ radical ion pair state, the **PTZP** π-radical cation (**PTZP**$^{\bullet+}$), which is formed within 25 ns, is corroborated by its fingerprint absorption[25] that includes a 500 nm maximum and a 400 nm minimum. When comparing the charge recombination in **DMAP-Pc1-C_{60}A** with

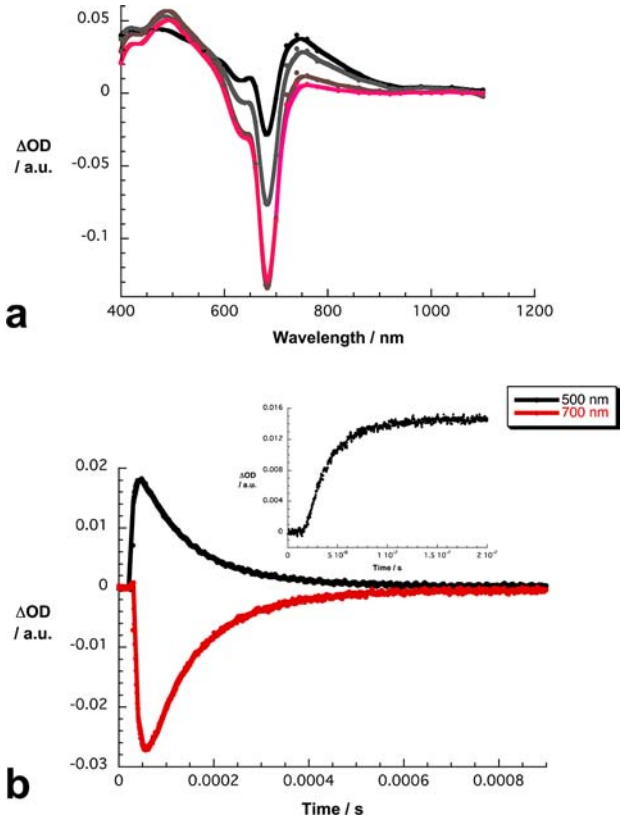

Figure 5. (a) Differential absorption spectra (visible and near-IR) obtained upon nanosecond flash photolysis (532 nm) of **PTZP-Pc1-C_{60}A** (4:1:4) in deaerated toluene with time delays of 6.1×10^{-6} s (black spectrum), 9.7×10^{-6} s (gray spectrum), 2.3×10^{-5} s (brown spectrum), and 4.0×10^{-5} s (red spectrum) at room temperature. (b) Time absorption profiles of the spectra shown above at 500 nm (**PTZP** radical cation) and 700 nm (**Pc1** triplet excited state) monitoring the charge recombination. The inset shows a zoom into the short time domain at 500 nm monitoring the charge shift.

the charge shift in **PTZP-Pc1-C_{60}A**, we derive an overall efficiency of 40%. Please note that the triplet excited state of **Pc1** evolves in competition with the charge shift.[26] Lifetimes of 7.5 μs (Figure S17, Supporting Information) and 110 μs were derived for the charge recombination and the triplet excited state decay, in the absence of any oxygen. When oxygen is present, the lifetimes are 60 and 110 ns due to activation- and diffusion-controlled processes, respectively.

3. CONCLUSIONS

In summary, we have demonstrated the formation of supramolecular three-component systems via an "all or nothing" process, where the synergistic coupling of two noncovalent binding equilibria, acting at different sites of **Pc1**, dissociates a robust Pc dimer, namely (**Pc1**)$_2$. Only when the two binding ligands, that is either C_{60}**A** and **DMAP** or C_{60}**A** and **PTZP**, are present, the activity of the system is turned on. As a result, a cascade of light-harvesting and electron-transfer processes, ultimately affording the **DMAP-Pc1**$^{\bullet+}$**-C_{60}A**$^{\bullet-}$ and **PTZP**$^{\bullet+}$**-Pc1-C_{60}A**$^{\bullet-}$ radical ion pair states, respectively, is noted. The latter is formed via a thermodynamically driven charge shift reaction in the initially formed **PTZP-Pc1**$^{\bullet+}$**-C_{60}A**$^{\bullet-}$ radical ion pair state that features lifetimes notably longer than those displayed by the corresponding **DMAP-Pc1**$^{\bullet+}$**-C_{60}A**$^{\bullet-}$ radical ion pair state.

dx.doi.org/10.1021/ja410114d | J. Am. Chem. Soc. 2013, 135, 19311−19318

■ ASSOCIATED CONTENT

Supporting Information

Text and figures giving synthesis and characterization details, additional self-assembly (Figures S1−S8), and photophysics data (Figures S9−S16). This material is available free of charge via the Internet at http://pubs.acs.org.

■ AUTHOR INFORMATION

Corresponding Author

tomas.torres@uam.es; dirk.guldi@fau.de; david.gonzalez.rodriguez@uam.es

Present Address

[‖]Institute for Complex Molecular Systems and Laboratory of Macromolecular and Organic Chemistry, Eindhoven University of Technology, P.O. Box 513, 5600 MB Eindhoven, The Netherlands.

Notes

The authors declare no competing financial interest.

■ ACKNOWLEDGMENTS

Funding from the MICINN and MEC (Spain) (CTQ-2011-24187/BQU and CTQ-2011-23659), Consolider-Ingenio Nanociencia Molecular (CSD2007-00010), Comunidad de Madrid (MADRISOLAR-2, S2009/PPQ/1533), the Bayerische Staatsregierung as part of the "Solar Technologies go Hybrid" initiative, and the Office of Basic Energy Sciences of the U.S. Department of Energy is acknowledged.

■ REFERENCES

(1) (a) Focus Issue on Cooperativity: *Nat. Chem. Biol.* **2008**, *4*, 433−507. (b) Hunter, C. A.; Anderson, H. L. *Angew. Chem., Int. Ed.* **2009**, *48*, 7488−7499. (c) Ercolani, G.; Schiaffino, L. *Angew. Chem., Int. Ed.* **2011**, *50*, 1762−1768.

(2) Eaton, W. A.; Henry, E. R.; Hofrichter, J.; Mozzarelli, A. *Nat. Struct. Biol.* **1999**, *6*, 351−358.

(3) (a) Carlson, S. W.; Branden, M.; Voss, K.; Sun, Q.; Rankin, C. A.; Gamblin, T. C. *Biochemistry* **2007**, *46*, 8838−8849. (b) Miraldi, E. R.; Thomas, P. J.; Romberg, L. *Biophys. J.* **2008**, *95*, 2470−2486. (c) Rice, L. M.; Montabana, E. A.; Agard, D. A. *Proc. Natl. Acad. Sci. U.S.A.* **2008**, *105*, 5378−5383 and references therein.

(4) (a) Yu, P.; Pettigrew, D. W. *Biochemistry* **2003**, *42*, 4243−4252. (b) Jaffe, E. K. *Trends Biochem. Sci.* **2005**, *30*, 490−497. (c) Durroux, T. *Trends Pharmacol. Sci.* **2005**, *26*, 376−384.

(5) (a) Kovbasyuk, L.; Krämer, R. *Chem. Rev.* **2004**, *104*, 3161−3187. (b) Gianneschi, N. C.; Masar, M. S., III; Mirkin, C. A. *Acc. Chem. Res.* **2005**, *38*, 825−837. (c) Zahn, S.; Reckien, W.; Kirchner, B.; Staats, H.; Matthey, J.; Lützen, A. *Chem. Eur. J.* **2009**, *15*, 2572−2580. (d) Yoon, H. J.; Kuwabara, J.; Kim, J.-H.; Mirkin, C. A. *Science* **2010**, *330*, 66−69.

(6) See, for example: (a) Martínez-Díaz, M. V.; Torres, T. In *Handbook of Porphyrin Science*; Kadish, K. M., Smith, K. M., Guilard, R., Eds.; World Scientific: Singapore, 2010; Vol. *10*, Chapter 45. (b) Fukuzumi, S. In *Handbook of Porphyrin Science*; Kadish, K. M.; Smith, K. M., Guilard, R., Eds.; World Scientific: Singapore, 2010; Vol. *10*, Chapter 46. (c) Martínez-Díaz, M. V.; de la Torre, G.; Torres, T. *Chem. Commun.* **2010**, *46*, 7090−7108. (d) Bottari, G.; Trukhina, O.; Ince, M.; Torres, T. *Coord. Chem. Rev.* **2012**, *256*, 2453−2477.

(7) (a) Bottari, G.; de la Torre, G.; M. Guldi, D.; Torres, T. *Chem. Rev.* **2010**, *110*, 6768−6816. (b) de la Torre, G.; Bottari, G.; Sekita, M.; Hausmann, A.; Guldi, D. M.; Torres, T. *Chem. Soc. Rev.* **2013**, *42*, 8049−8105. (c) Ragoussi, M.-E.; Ince, M.; Torres, T. *Eur. J. Org. Chem.* **2013**, 6475−6489. (d) Cioffi, C.; Campidelli, S.; Sooambar, C.; Marcaccio, M.; Marcolongo, G.; Meneghetti, M.; Paolucci, D.; Paolucci, F.; Ehli, C.; Rahman, G. M. A.; Guldi, D. M.; Prato, M. *J. Am. Chem. Soc.* **2007**, *129*, 3938−3945. (e) Mateo-Alonso, A.; Guldi, D. M.; Paolucci, F.; Prato, M. *Angew. Chem. Int. Ed.* **2007**, *46*, 8120−8126.

(8) (a) Häder, D. P. *Photosynthese*, 1st ed.; Thieme: Stuttgart, New York, 1999. (b) Stryer, L. *Biochemistry*, 4th ed.; W. H. Freeman: New York, 1995.

(9) Martinez-Díaz, M. V.; Díaz, D. D. *J. Porphyrins Phthalocyanines* **2009**, *13*, 369.

(10) Segura, M.; Sánchez, L.; de Mendoza, J.; Martín, N.; Guldi, D. M. *J. Am. Chem. Soc.* **2003**, *125*, 15093.

(11) Engelhardt, V.; Kuhri, S.; Fleischhauer, J.; García-Iglesias, M.; González-Rodríguez, D.; Bottari, G.; Torres, T.; Guldi, D. M.; Faust, R. *Chem. Sci.* **2013**, 3888−3893.

(12) **Pc1** dimers are actually a mixture of two isomers with "oblique" and "parallel" relative ZnPc arrangements (see also ref 13 and Figure S4 (Supporting Information)).

(13) Kameyama, K.; Morisue, M.; Satake, A.; Kobuke, Y. *Angew. Chem., Int. Ed.* **2005**, *44*, 4763−4766.

(14) However, an additional red-shifted low-intensity band is seen at 788 nm immediately after dissolving **Pc1** samples in toluene. This band vanishes within a few hours in room-temperature solutions (see Figure S5, Supporting Information). Its disappearance is accelerated at higher temperatures or on adding small amounts of more polar solvents or pyridine ligands. We believe this band corresponds to supramolecular oligomeric species of **Pc1** that are kinetically trapped in the solid state and slowly interconvert to the thermodynamically stable dimer in diluted samples. These oligomeric species were also detected in MS experiments.

(15) The fluorescence quantum yield of a tetra-*tert*-butyl ZnPc reference is 0.3.

(16) (a) D'Souza, F.; Ito, O. *Chem. Commun.* **2009**, 9413−9428. (b) Maligaspe, E.; Kumpulainen, T.; Lemmetyinen, H.; Tkachenko, N. V.; Subbaiyan, N. K.; Zandler, M. E.; D'Souza, F. *J. Phys. Chem. A* **2010**, *114*, 268−277. (c) Bandi, V.; El-Khouly, M. E.; Nesterov, V. N.; Karr, P. A.; Fukuzumi, S.; D'Souza, F. *J. Phys. Chem. C* **2013**, *117*, 5638−5649.

(17) In the case of the amidinium-carboxylate association, binding constants are extremely sensitive to solvent polarity. See: (a) Kirby, J. P.; Roberts, J. A.; Nocera, D. G. *J. Am. Chem. Soc.* **1997**, *119*, 9230−9236. (b) Orner, B. P.; Salvatella, X.; Sánchez-Quesada, J.; de Mendoza, J.; Giralt, E.; Hamilton, A. D. *Angew. Chem., Int. Ed.* **2002**, *41*, 117−119. (c) Otsuki, J.; Kanazawa, Y.; Kaito, A.; Islam, D. M. S.; Araki, Y.; Ito, O. *Chem. Eur. J.* **2008**, *14*, 3776−3784. (d) Ito, H.; Ikeda, M.; Hasegawa, T.; Furusho, Y.; Yashima, E. *J. Am. Chem. Soc.* **2011**, *133*, 3419−3432.

(18) (a) Rosenthal, J.; Hodgkiss, J. M.; Young, E. R.; Nocera, D. G. *J. Am. Chem. Soc.* **2006**, *128*, 10474−10483. (b) Sánchez, L.; Sierra, M.; Martín, N.; Myles, A. J.; Rebek, J. D., Jr.; Seitz, W.; Guldi, D. M. *Angew. Chem., Int. Ed.* **2006**, *45*, 4637−4641. (c) Young, E. R.; Rosenthal, J.; Hodgkiss, J. M.; Nocera, D. G. *J. Am. Chem. Soc.* **2009**, *131*, 7678−7684.

(19) A rough estimation of the association constant of $(\mathbf{Pc1})_2$ with pyridine and carboxylic acid ligands afforded a value: $K_T \approx 10^5\ M^{-1}$ (Figure S7, Supporting Information).

(20) See the Supporting Information for further details.

(21) (a) Thomas, K. G.; Biju, V.; George, M. V.; Guldi, D. M.; Kamat, P. V. *J. Phys. Chem. A* **1998**, *102*, 5341−5348. (b) Foley, S.; Bosi, S.; Larroque, C.; Prato, M.; Janot, J.-M.; Seta, P. *Chem. Phys. Lett.* **2001**, *350*, 198−205. (c) Lee, M.; Song, O. K.; Seo, J. C.; Kim, D.; Suh, Y. D.; Jin, S. M.; Kim, S. K. *Chem. Phys. Lett.* **1992**, *196*, 325. (d) Ebbesen, T. W.; Tanigaki, K.; Kuoshima, S. *Chem. Phys. Lett.* **1991**, *181*, 501. (e) Foote, C. S. *Top. Curr. Chem.* **1994**, *169*, 347−363.

(22) (a) Biju, V.; Barazzouk, S.; Thomas, K. G.; George, M. V.; Kamat, P. V. *Langmuir* **2001**, *17*, 2930−2936. (b) Díaz, M. C.; Herranz, M. A.; Illescas, B. M.; Martín, N.; Godbert, N.; Bryce, M. R.; Luo, C.; Swartz, A.; Anderson, G.; Guldi, D. M. *J. Org. Chem.* **2003**, *68*, 7711−7721.

(23) Changing the C_{60} concentration exerted no noticeable impact on the charge separation dynamics. Only the relative yields of $C_{60}^{\bullet-}$ varied in proportion to the C_{60} concentration.

(24) The charge shift reaction is thermodynamically favored when comparing the ZnPc and the phenothiazine oxidation potentials of 0.19 and 0.15 V versus Fc^{+}/Fc, respectively.
(25) Kawauchi, H.; Suzuki, S.; Kozaki, M.; Okada, K.; Islam, D. M. S.; Araki, Y.; Ito, O.; Yamanaka, K. *J. Phys. Chem. A* **2008**, *112*, 5878−5884.
(26) Simulation of the dynamic processes with ACUCHEM[27] resulted in rate constants for the charge recombination process to yield the ZnPc triplet excited state of $(5 \pm 1) \times 10^{5}$ s^{-1} and its decay of $(0.85 \pm 0.2) \times 10^{4}$ s^{-1}.
(27) Braun, W.; Herron, J. T.; Kahaner, D. K. *Int. J. Chem. Kinet.* **1988**, *20*, 51−62.